International Journal of Applied Science and Engineering

Behavior of reinforced concrete beams cast with a proposed geopolymer concrete (GPC) mix

Rami A. Hawileh, Haitham A. Badrawi, Hisham Y. Makahleh, Abdul Saboor Karzad*, Jamal A. Abdalla

Department of Civil Engineering, American University of Sharjah, P.O.BOX 26666, Sharjah, UAE

ABSTRACT

The aim of this paper is to examine the effects of using Ground Granulated Blast Furnace Slag (GGBFS) as a complete replacement to Ordinary Portland Cement (OPC) in Reinforced Concrete (RC) beams. The proposed GGBFS mix had an air content of 1.4%, a unit weight of 2480 kg/m^3, a slump of 201 mm, and a compressive strength of 30 MPa after 56 days of curing. In addition, the GGBFS-based sample have shown an increased durability as it passed less chloride ions when compared to conventional concrete. A total of four beams were cast using the proposed mix and then tested under three-point loading and four-point loading. The beams were categorized into group 1, samples designed to fail in flexure, and group 2, samples designed to fail in shear. The performances of the GGBFS-based specimens were evaluated and compared to the control beams. In flexure, the GGBFS-based sample carried 83% of the control sample's ultimate load which is considerably less than the expected 96%. Whereas the GGBFS-based shear deficient sample carried 79% of the load carried by the control beam. Although GGBFS samples carried less load, it is concluded that use of GGBFS as a full replacement to OPC is practical as the normalized capacity of GGBFS samples is comparable to that of the control samples. Additionally, using GGBFS contributes to the reduction of CO_2 emissions and hence promotes the use of sustainable and green concrete.

Keywords: Compressive strength, Flexure, Shear, Concrete, Geopolymer concrete, GGBFS.

OPEN ACCESS

Received: February 12, 2022
Revised: May 27, 2022
Accepted: May 30, 2022

Corresponding Author:
Abdul Saboor Karzad
karzad@live.com

Publisher:
Chaoyang University of Technology
ISSN: 1727-2394 (Print)
ISSN: 1727-7841 (Online)

1. INTRODUCTION

The concern about the environmental impacts of the materials used in construction has grown rapidly in recent decades. Ordinary Portland Cement (OPC) is one of the primary materials used in forming Reinforced Concrete (RC) structures. The global production of OPC has increased rapidly in recent years (Andrew, 2018). This is because OPC has been extensively used in construction. Nonetheless, it contributes to approximately 5-7% of annual anthropogenic global CO_2 emissions and hence causes greenhouse effect (Turner and Collins, 2013; Huntzinger and Eatmon, 2009). Moreover, the production of OPC is associated with the continuous depletion of the ozone layer and global warming. Therefore, there is an urgent need to reduce OPC related CO_2 emissions and explore potential eco-friendly alternatives.

Ground Granulated Blast Furnace Slag (GGBFS) is an alternative material to OPC in concrete mix that is less energy intensive and has lower carbon emissions (Andrew, 2018). GGBFS is a by-product from blast-furnace in water or steam used to make iron. It is produced from placing the mixture of iron-ore, coke, and limestone in blast furnace at about 1500^{O}C temperatures. The products of this mixture are molten iron and molten slag (Saranya et al., 2018). The molten is less dense and formulates a layer above the molten iron. Thus, molten slag is channelled out of the furnace as a molten lava and can be separated in the skimmer. Subsequently, GGBFS is formulated by quick quenching of the cooled molten slag using high pressure water jets. The particles are then dried and ground to produce very fine powder of GGBFS (Yuksel, 2018). The chemical composition of GGBFS is compromised from Al_2O_3, CaO and SiO_2 and has two phases, glassy and crystalline (Grist et al., 2015). The glassy phase is responsible for its cementitious properties, while the crystalline phase is mainly responsible for hydration (Wu et al., 2015; Nagaratnam et al., 2016).

Based on its physical and chemical compositions, GGBFS-based concrete mixes has better mechanical properties, durability, and corrosion resistance compared to OPC-based concrete (Oner and Akyuz, 2007; Ma et al., 2018; Cheng et al., 2005). According to an experimental study on the optimum usage of GGBFS for the compressive strength performed by Oner and Akyuz, (2007), the compressive strength of concrete mixtures containing GGBFS increases as the amount of GGBFS increases till it reaches the optimum point at around 55% of the total binder content. Moreover, based on a study conducted by Sangeetha and Joanna (2015), the flexural behaviour of GGBFS RC beams is comparable to that of OPC RC beams. In an experimental study performed by Babu and Kumar (2000), load-deflection characteristics, crack patterns, and failure modes observed for GGBFS RC beams were found to be comparable to that of OPC RC beams.

In 2015, Crossin studied the greenhouse gas implications of using GGBFS as a cement alternative. His results indicate using GGBFS as cement substitute decreases greenhouse gases by 47.5%. A study involving the use of GGBFS as an alternative binder to OPC illustrated greater durability and corrosion resistance for the GGBFS binder (Ma, 2018; Crossin, 2015; Yeau et al., 2005). According to the literature, GGBFS showed a relatively lower cementitious property compared to OPC because the activation of GGBFS in alkaline conditions decreases the total hydration products of cement. As a result, GGBFS provides sufficient spacing to uniformly distribute the hydration products of cement and therefore impacts the total strength of concrete (Ramakrishnan et al., 2017).

Several studies have shown that 50% replacement of OPC with GGBFS resulted in higher durability, strength, and strength gain of RC (Wan et al., 2004; Jeong et al., 2017; Babu and Kumar, 2000). In certain situations, such as hostile and harsh conditions, OPC can be replaced with up to 85% of GGBFS to produce concrete (Samad et al., 2017; Siddique, 2013). Furthermore, a study investigated the use of GGBFS in harsh wastewater conditions concluded that partial replacement of OPC with GGBFS enhanced the performance of concrete in terms of increasing resistance to sulphate attacks and hence diminishing the deterioration of concrete (Siddique, 2012). Concrete deterioration that leads to a failure in construction is caused by the corrosion of steel in RC. GGBFS and silica fume have substantially demonstrated to increase the corrosion resistance of steel in RC (O'Connell et al., 2012; Topçu and Ahmet, 2010).

Although using GGBFS as form of replacement to OPC has many advantages, there are still some disadvantages. Generally, using GGBFS reduces the overall workability, has less early strength gain, and increases dry shrinkage coefficient (Garcia-Lodeiro et al., 2015; Junaid. et al., 2020). In addition, high quantities of SiO_2 in concrete mixes causes pozzolanic reaction and delays the setting times (Eguchi et al., 2013; Allahverdi et al., 2018). Thus, concrete mixes containing GGBFS and OPC require additional water for workability (Nagaratnam et al., 2016). Nonetheless, adding more water decreases the total strength of concrete.

The literature is lacking relevant experimental research on testing RC beams with higher percentages of GGBFS as a replacement to cement in concrete mixes (Thomas et al., 2021; Hamada et al., 2021; Hawileh et al., 2017; Nawaz et al., 2019). Even though several studies investigated the effects of partial replacement of OPC with GGBFS on the behaviour of RC beams. Nonetheless, few studies assessed the effect of substituting OPC with GGBFS and different proposed mix. Therefore, this paper examines the effects of using GGBFS as a full replacement to OPC in RC beams. In this experiment, a total of four RC beams, two with full replacement of OPC with GGBFS and two serving as control samples with 100% OPC as binder, were tested under three-point and four-point loading. The test results include the midspan deflection response curves, load-carrying capacity, ductility, and failure mode. In addition, standard tests were conducted to examine the fresh and hardened concrete properties for both mixes.

2. MATERIALS AND METHODS

In this study, the effects of full replacement of OPC with GGBFS on the behaviour of RC beams are investigated. A concrete mix using 100% OPC as binder serves as a control mix while a geopolymer concrete (GPC) is designed using 100% GGBFS as binder. First, fresh concrete properties are investigated for both mixes. In addition, cubes, cylinders, and prisms are used to investigate mechanical properties of hardened concrete and lastly RC beams cast using the same mix were tested for shear and flexure behaviour. A total of four beams were tested under three-point and four-point loading in simply supported condition. The physical and mechanical properties of the materials used, concrete mix proportioning, detailing of the tested beam specimens, and test setups are described in the following subsections.

2.1 Materials

2.1.1 OPC and GGBFS

Binder materials (GGBFS and OPC) used in this research were obtained from the Sharjah Cement Factory. Table 1 shows the chemical composition of the binding material used.

Table 1. Chemical compositions of OPC and GGBFS (%)

Binder	SiO_2	Al_2O_3	Fe_2O_3	CaO	MgO	SO_3	Na_2O	Cl^-	LOI*	Fineness kg/m^2
OPC	20.70	5.40	3.86	63.22	0.99	2.62	0.56	0.02	2.89	346
GGBFS	34.90	14.46	0.60	39.80	6.00	0.10	0.55	0.02	1.67	430

* LOI: Loss on Ignition

2.1.2 Water

The water used in concrete mixing has the properties shown in Table 2 as reported by Al Futtaim Element Lab.

Table 2. Water properties

Property	Units	Value
pH	pH units	370
Total Dissolved Solids	mg/L	171
Bicarbonate	mg/L	32
Carbonate	mg/L	5
Total Alkalinity	mg/L	34
Sulphate	mg/L	< 5
Chloride	mg/L	74.0

2.1.3 Reinforcing Steel

Reinforcement used in the beams is A706 low-alloy grade 420 deformed steel bars that is produced in the United Arab Emirates and have the properties summarized in Table 3. Reinforcing steel rebars and shear stirrups are supplied by TransGulf Ready Mix Company.

2.1.4 Aggregates

Four different types of aggregates, 20 mm coarse crushed aggregate, 10 mm coarse crushed aggregate, 0-5 mm sand crushed aggregate, and 0.6 mm dune sand, were used. Al Futtaim Element Lab reported the properties of the aggregates as shown in Table 4.

Table 3. Properties of reinforcing steel

Reinforcing steel	Type	Grade	Yield strength (MPa)	Diameter (mm)
Longitudinal	Deformed A706 low-alloy	420	590	8 & 12
Stirrups	Deformed A706 low-alloy	420	590	8

Table 4. Properties of aggregates

Aggregates	Particle density SSD (kg/m^3)	Sand equivalent value (%)	Water absorption (%)	Los Angeles abrasion value (%)	Material finer than 75-micron (%)
0.6 mm Dune Sand	2650	79	0.7	-	1.9
0-5 mm Dune Sand	2690	79	0.5	-	4.4
10 mm Crushed Aggregate	2820	-	0.4	17	0.3
20 mm Crushed Aggregate	2810	-	0.3	19	0.1

2.2 Concrete Mix Proportioning

Two concrete mixes are prepared: the control mix with 100% OPC as binder while the other contains GGBFS as a full replacement of OPC. Table 5 shows the mix proportioning for both the mixes. The admixture is only added to the control mix while alkaline activator is only used in the GGBFS mix concrete. The mixes are designed to achieve a concrete compressive strength of 30 MPa at the age of 28 days.

Table 5. Mix proportioning

	Control mix (100% OPC)	100% GGBFS mix
OPC dosage ratio	1.0	0.0
GGBFS dosage ratio	0	1.0
OPC (kg/m^3)	370	0
GGBFS (kg/m^3)	0	370
Water (L/m^3)	170	170
W/C Ratio	0.46	0.46
Coarse Aggregates (kg/m^3)	1007	1007
Fine Aggregates (kg/m^3)	893	893
Admixture (L/m^3)	4	-
Alkaline Activator (L/m^3)	-	14.5

2.3 Test specimens and setup

Two RC beams, labelled as group 1 (designations of the beam specimens are given in Table 6) and designed to fail in flexure are tested under a four-point loading setup after 56 days curing. Beams are reinforced with tension steel that is composed of two No. 12 bars with an area of 113.1 mm^2 that makes up 2.83% of the concrete section.

Both beams have a width of 150 mm, a span of 1700 mm, and a height of 300 mm and are reinforced with shear stirrups internally throughout their entire lengths as seen in

Figs. 1 and 2. The test setup is show in Fig. 3, representing simply supported beams tested under load control mode with a loading rate of 150 newtons per second.

Two RC beams labelled as group 2 (designations of the beam specimens are given in Table 6) and designed to fail in shear are tested under a three-point loading setup after 56 days of curing. The samples have a width of 150 mm, a span of 1700 mm, a height of 300 mm, are reinforced internally by shear reinforcement stirrups over one half of the span of the beam to ensure a shear failure of the beam over the non-reinforced span and have a shear span to depth ratio of 3.58. Tension steel reinforcement is composed of two No. 12 bars with an area of 113.1 mm^2 which makes up 2.83% of the concrete section. Fig. 4, Fig. 5 and Fig. 6 illustrate the detailing of the tested specimens. The test setup shown in Fig. 7, represents simply supported beams tested under load control mode with a loading rate of 150 newtons per second.

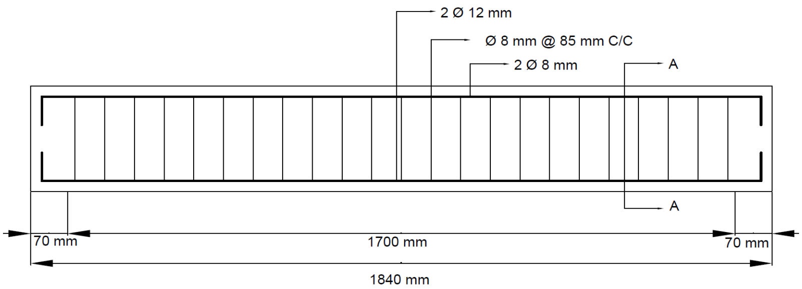

Fig. 1. Flexural strength test (group 1) specimen side view

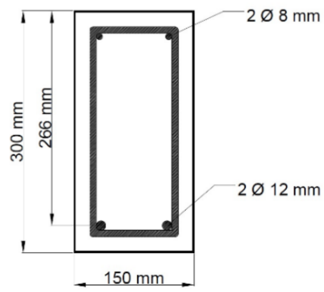

Fig. 2. Group 1 samples section A-A

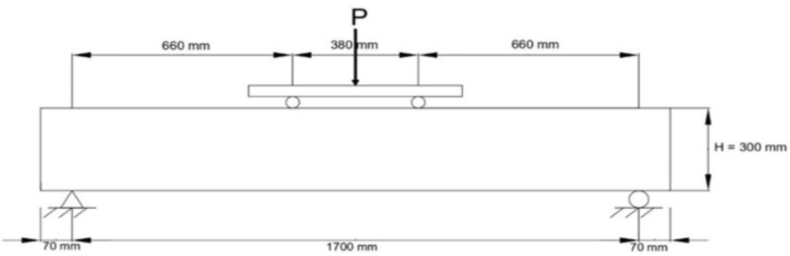

Fig. 3. Flexural strength test setup

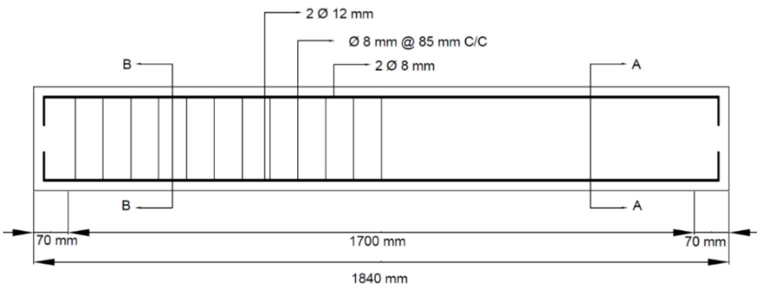

Fig. 4. Shear strength test (group 2) specimen side view

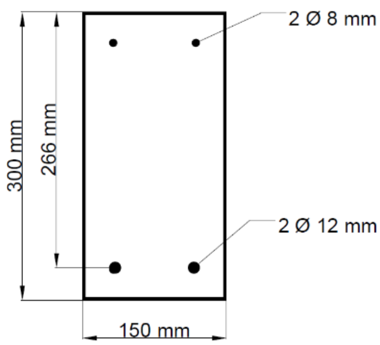

Fig. 5. Group 2 sample section A-A

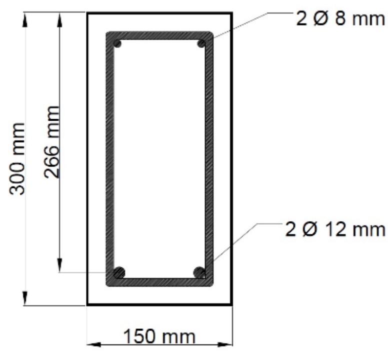

Fig. 6. Group 2 sample section B-B

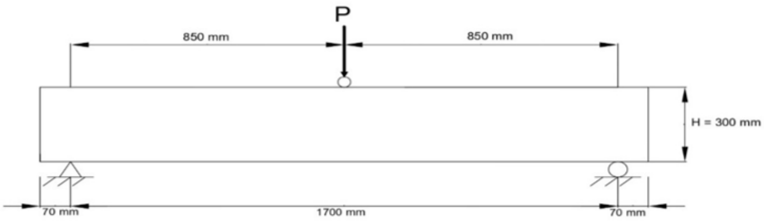

Fig. 7. Shear strength test setup

Table 6. Test matrix

Beam Designation	Description	Number of samples
G1_BC	Control Beam tested for flexure with 100% OPC	1
G1_BG	Beam tested for flexure with 100% GGBFS	1
G2_BC	Control Beam tested for shear with 100% OPC	1
G2_BG	Beam tested for shear with 100% GGBFS	1

3. RESULTS AND DISCUSSION

3.1 Properties of Fresh Concrete

The workability of the control mix and the GGBFS-based mix, tested following ASTM C143, was found having true slump (180-220 mm) as shown in Table 7. In addition, air content for the control mix and GGBFS-based mix are consecutively 1.2, and 1.4 which are within the required limits of ASTM C231 (1% - 2%). Lastly, the unit weight results obtained for the control mix and GGBFS-based mix are 2480 kg/m^3, and 2450 kg/m^3 respectively which are within the acceptable range between 2400 kg/m^3 to 2600 kg/m^3.

Table 7. Fresh concrete test results

Property	Control mix (100% OPC)	100% GGBFS mix
Workability (mm)	201	180
Air Content (%)	1.2	1.4
Unit Weight (kg/m^3)	2480	2450

3.2 Mechanical Properties of Hardened Concrete

3.2.1 Compressive Strength

The compressive strengths of both concrete mixes obtained by testing cube samples following ASTM C39 testing procedure at 7, 28, and 56 days are summarized in Table 8. It is noticed that the control mix reached the design compressive strength within 7 days of curing while the GGBFS-based mix reached 65% of its design compressive strength during the same period. The compressive strength gain of GGBFS samples is comparable to that of experiment conducted by Oner and Akyuz (2007). Notably, the compressive strength ratio of GGBFS based sample to that of OPC was around 0.50 within the first 28 days of curing. However, after testing the 56-days-curing samples, the GGBFS-based mix gained a higher proportion of compressive strength due to the late setting of the mix and the longer period of curing required. In addition, it is expected that the GGBFS mix will gain more strength when cured more than 56 days considering the observed pattern of strength gain. Moreover, the compressive strength of both mixes was evaluated using standard cylinders following BS 1881 Part 116 testing procedure after 28 days curing to determine the compressive strength that was later used in the calculations of flexural and shear strengths of RC beams. The control mix reached a strength of 32.6 MPa while the GGBFS-based mix reached a strength of 20.2 MPa. Comparing the two values, the GGBFS-based mix provided 62% of the strength provided by the control mix.

3.2.2 Split Tensile Strength

The tensile strength of tested specimen at 28 days of curing following ASTM C496 split-tension test was 3.1 MPa and 1.9 MPa for the control mix and GGBFS-based mix respectively. Table 8 shows the results of split tensile test.

3.2.3 Modulus of Rupture

Following the ASTM C78 testing procedure, the modulus of rupture of the control mix after 28 and 56 days was 4.2 MPa and 5.5 MPa respectively. Whereas the GGBFS-based mix reached a stress of 2.5 MPa, and 2.6 MPa after 28 and 56 days respectively before failing. The ratio of strength of the two mixes was 0.6 at the 28-days-curing, however, it decreased to 0.47 at the 56-days-cured sample. Table 8 shows the modulus of rupture results.

3.2.4 Durability

The ASTM C1202 Rapid Chloride Permeability Test was conducted on 2 cube samples for each mix after 28 and 56 days. The control mix passed 4375 and 3122 Columbs after 28 and 56 days while the GGBFS-based mix passed only 1069 and 879 Columbs after the same curing periods. Comparing the two mixes, the GGBFS binder produced a highly durable concrete that passed only around 25% of the charge that passed through the conventional concrete. This indicates that replacing OPC with GGBFS increases durability drastically. Table 8 summarizes the RCP test results.

The results obtained from this experiment draws upon literature and better assist the impacts of GGBFS as a replacement to OPC. Moreover, the outcomes of this experiment confirm the findings of previous research conducted by Wan et al. (2004), Jeong et al. (2017), and Babu and Kumar (2000).

Table 8. Mechanical properties of concrete

Test	Curing (Days)	Control mix (100% OPC)	100% GGBFS mix	GGBFS/OPC
Compressive strength (MPa), cubes	7	38.8	19.8	0.51
	28	49.8	24.8	0.50
	56	54.0	30.0	0.56
Compressive strength (MPa), cylinders	28	32.6	20.2	0.62
Split tensile strength (MPa)	28	3.1	1.9	0.61
Modulus of rupture (MPa)	28	4.2	2.5	0.60
	56	5.5	2.6	0.47
Rapid chloride permeability (col)	28	4375	1069	0.24
	56	3122	879	0.26

3.3 Behavior of RC Beams

3.3.1 Flexural Behavior

As seen in Fig. 8, the samples were tested under a four-point loading test setup. Fig. 9 shows the failed RC beam specimens. After loading the beams, the tension reinforcement of the control sample and the GGBFS-based sample yielded at a load, Py, of 108.37 kN and 90.78 kN respectively. Hawileh et al. (2017) obtained a tension reinforcement yield load Py, of 70.17 kN for the control sample and 67.09 kN for the GGBFS sample (90% replacement of OPC). Moreover, the control and the GGBFS-based samples reached an ultimate load, Pu, of 124.05 kN and 103.00 kN respectively. Finally, the control sample's failure load, P_f, was 105.32 kN and the GGBFS-based sample's failure load was 80.24 kN.

3.3.1.1 Failure Mode of The Tested Specimens

As expected and consistent with the literature (Hawileh et al., 2017), the tested beam specimens failed in the desirable tension-controlled failure mode by yielding of the flexural steel reinforcement followed by concrete crushing in the top compression zone as seen in Fig. 9. Noticeably, the failure was a flexural failure in both samples as the shear resistance provided by the concrete section was more than the load at which both samples failed.

3.3.1.2 Load-Deflection of Beam Specimens

The ductility of the geopolymer concrete sample is compared with the control sample. As seen in Fig. 10, the load versus mid-span deflection is plotted and at yielding, the control and the GGBFS-based samples witnessed a deflection of 7.93 mm and 8.66 mm respectively. This observation points out that the GGBFS mix sample provides higher ductility than the control sample. The deflections of the samples at ultimate loads were 23.93 mm and 29.99 mm for the control and GGBFS-based samples respectively and that supports the indication that the GGBFS-based sample is more ductile. Furthermore, as seen in Table 9, the ductility of the beam specimens is evaluated by computing the ductility index, μ, which corresponds to the ratio of midspan deflection at ultimate load, δu to δy that corresponds to deflection at yielding of the steel reinforcement. For the control sample μ was 3.01 and 3.46 for the GGBFS-based sample. This indicates that GGBFS-based concrete beam exhibits more ductility than the concrete using OPC as binder.

Table 9. Deflection and ductility index results

Specimen ID	δu (mm)	δy (mm)	δf (mm)	μ (δu/ δy)
G1_BC	23.93	7.93	27.42	3.01
G1_BG	29.99	8.66	53.91	3.46

Moreover, to account for the variability in the compressive strength of both mixes which ranged from 20.22 to 32.59 MPa, the flexural load, on the vertical axis, was normalized by the square root of the compressive strength as illustrated in Fig. 11. This is done because compressive strength variability can impact the cracking response of the beams and thus the overall behavior of the specimens. Comparing the normalized curves, it is observed that the geopolymer concrete sample performed better than the control sample.

Similarly, as seen in Fig. 12 which shows the longitudinal strain in the flexural reinforcement measured by strain gauges, the strain in GGBFS-based sample's tension steel has reached around 0.015 strain while the strain reading of the steel in the control sample reached less than 0.007 strain which also proves the higher ductility in the geopolymer concrete sample. The flexural behaviour of the GGBFS samples is similar to that of the experiment conducted by Sangeetha and Joanna (2015).

A. G1_BC sample B. G1_BG sample

Fig. 8. Specimens under testing

A. G1_BC sample B. G1_BG sample

Fig. 9. Tested specimens after failure

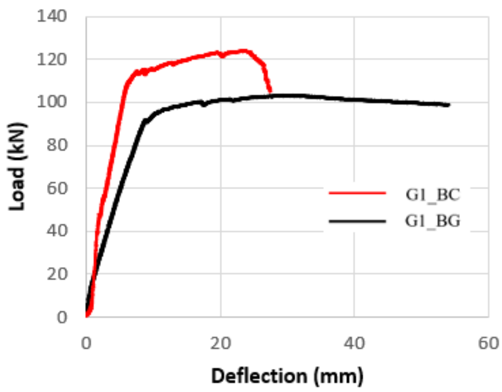

Fig. 10. Load versus mid-span deflection response curves for flexural dominant samples

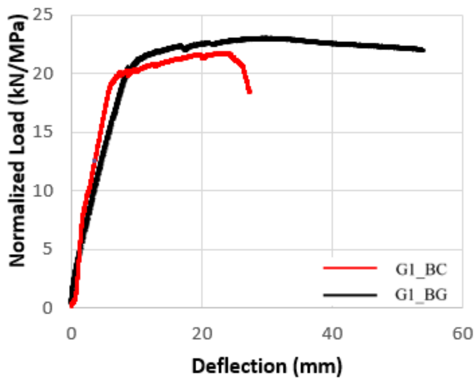

Fig. 11. Normalized load vs mid-span deflection response for flexural dominant samples

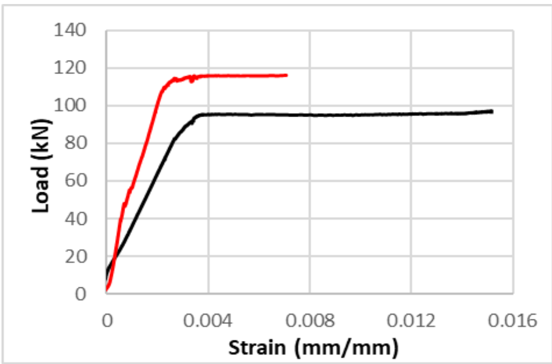

Fig. 12. Load vs strain curves for flexural testing samples

3.3.2 Shear Behavior

As shown in Fig. 13, the samples were tested under a three-point loading test setup. Fig. 14 shows failed RC beam specimens after testing. As expected, the beam specimens failed in the desirable conventional mode of diagonal shear failure. From the test results of group 2 samples (summarized in Table 10), it is noticed that the control sample reached a maximum load of 82.16 kN at 6.21 mm and the GGBFS-based sample reached an ultimate load of 64.82 kN at 7.63 mm deflection. Moreover, the failure load was found to be 60.57 kN for the control sample while it was 51.86 kN for the GGBFS-based sample. When comparing the deflections at failure for both samples, it was found that the GGBFS-based sample exhibited more ductility with 8.91 mm deflection compared to 6.60 mm for the control sample. Fig. 15 depicts the load vs mid-span deflection response curves for the control and GGBFS based samples.

To account for the variability in the compressive strength of both mixes which ranged from 20.22 to 32.59 MPa, the shear load was normalized by the square root of the compressive strength as seen in Fig. 16. This is done because the variability in compressive strength can impact the cracking response of the beams thus the overall behavior of the specimens. When comparing the normalized curves, it is observed that the geopolymer concrete sample performance was comparable to that of the control sample but with more deflection before failure.

Table 10. Shear strength test results at 56 days

Specimen ID	Pu (kN)	δu (mm)	Pf (kN)	δf (mm)
G2_BC	82.16	6.21	60.57	6.60
G2_BG	64.82	7.63	51.86	8.91

A. G2_BC sample B. G2_BG sample

Fig. 13. Specimens at shear test setup

A. G2_BC sample B. G2_BG sample

Fig. 14. Tested specimens at shear failure

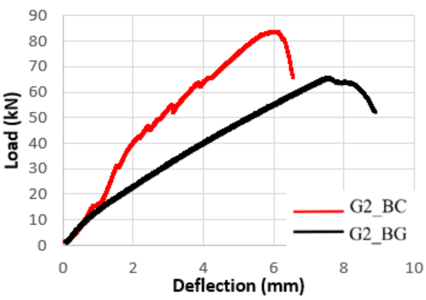

Fig. 15. Load versus mid-span deflection response curves for shear deficient samples

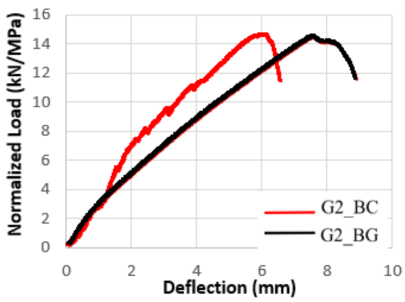

Fig. 16. Normalized load vs mid-span deflection response for shear defecient samples

4. ANALYTICAL PREDICTIONS USING ACI 318 DESIGN GUIDELINES

4.1 Flexural Strength

Using the ACI-318 code, the ultimate flexural capacities of the beams were calculated. The compressive strength used in predictions was 32.59 MPa for the control beam and 20.22 MPa for the GGBFS-based beam. The control beam was estimated to fail at an ultimate load of 98 kN while the GGBFS-based beam was predicted to fail at 94 kN applied load. After testing, the control beam failed at an ultimate load of 124 kN while the GGBFS-based concrete reached an ultimate load of 103 kN. Moreover, both samples performed better than expected. The predicted capacity for the control beam was 79% of the experimental value obtained. Similarly, the predicted capacity for the GGBFS-based beam was 91% of the experimental value obtained. Table 11 presents and compares the predicted and experimentally measured ultimate loads for both beams.

Table 11. Load-carrying capacity of flexural beams

Specimen	(Pu`) Experimental (kN)	(Pu) Predicted (kN)	(Pu) / (Pu`)
G1_BC	124	98	0.80
G1_BG	103	94	0.90

4.2 Shear Strength

Using the ACI-318 code, the shear capacities of the beams were calculated. The compressive strength used in calculations was 32.59 MPa for the control beam and 20.22 MPa for the GGBFS-based beam. The control beam and the GGBFS-based beam were estimated to fail in shear at an ultimate load of 77 and 61 kN, respectively. However, after testing, the control beam failed at an ultimate load of 82 kN and the GGBFS-based sample at 65 kN applied load. It was found that both samples performed better than expected, i.e., the predicted capacity was 94% of the experimental value obtained for both the control and the GGBFS-based samples. Table 12 presents the predicted and experimentally measured ultimate loads for both samples.

Table 12. Load-carrying capacity of shear deficient beams

Specimen	(Pu`) Experimental (kN)	(Pu) Predicted (kN)	(Pu) / (Pu`)
G2_BC	82	77	0.94
G2_BG	65	61	0.94

5. CONCLUSION

In this paper, a GGBFS concrete mix as an alternative to OPC concrete mix was developed and its properties was investigated. Mechanical properties of fresh and hardened proposed concrete mix was studied as per the commonly used test standards. In addition, full scale RC beam samples were cast to assess the flexural and shear behaviour of beams cast with such concrete mixes. From the investigation of test results, the following observations and conclusions were drawn:

1. The slump test result of the GGBFS mix was true with 180 mm slump. The air content was 1.4% which is within the acceptable range and finally, the unit weight was 2480 kg/m^3 implying normal weight concrete.
2. The design compressive strength of the GGBFS mix was achieved after 56 days of curing because of the late setting of geopolymer concrete as a result of the chemical activation of GGBFS.
3. The split tensile strength of the GGBFS-based concrete was 1.9 MPa after 28 days and 3.1 MPa for the control mix.
4. The modulus of rupture of GGBFS-based concrete was 2.6 MPa after 56 days which is 47% of the control mix strength.
5. The rapid chloride permeability test revealed that the use of GGBFS as binder enhances the durability of hardened concrete significantly.
6. Samples tested for flexure behavior failed by yielding of longitudinal tension reinforcement followed by concrete crushing in the top compression zone of the mid-span region.
7. Both samples performed better than predicted by ACI model, i.e., the predicted capacity for the control beam was 79% of the experimental value obtained and 91% for the GGBFS-based beam.
8. Both the OPC and GGBFS based shear deficient beam specimens failed in a diagonal shear failure mode.
9. Both concrete samples, tested for shear, performed better than the prediction by ACI model, i.e., the control and the GGBFS-based samples achieved 6% more load than predicted.

In summary, it is concluded that GGBFS can be used to produce geopolymer concrete which can serve as an acceptable alternative to ordinary concrete. That is because, it offers comparable results to that of the control mix in both fresh and hardened concrete properties. In addition, geopolymer concrete can be considered as a more sustainable concrete and that is due to the higher durability than that of OPC concrete.

It is recommended to test more beam samples with different parameters in future research studies to ensure that cement can be fully replaced with GGBFS or other supplementary cementitious materials.

ACKNOWLEDGMENT

The authors would like to thank TransGulf ReadyMix for supplying GGBFS, steel bars, Alkaline Activator, and casting of the RC beam specimens. The authors acknowledge the assistance and technical support of Eng. Ahmed Khartabil from TransGulf ReadyMix. The authors would also like to gratefully acknowledge Mr. Waleed Nawaz, Mr. Kais Douier, Ms. Nour Barakat, and Rami Assadi for their assistance and aid in conducting the tests.

REFERENCES

ACI Committee 318, 2014. Building code requirements for structural concrete and commentary, American Concrete Institute, Farmington Hills (MI)

Allahverdi, A. Maleki, A., Mahinroosta, M. 2018. Enhancement of hydraulic activity of slag-blended portland cement. Asian Journal of Civil Engineering, 19, 1009–1020.

Andrew, R. 2018. Global CO2 emissions from cement production, 1928–2017. Earth System Science Data, 10, 2213–2239.

Babu, K, Kumar, R. 2000. Efficiency of ggbs in concrete. Cement and Concrete Research, 30, 1031–1036.

Cheng, A., Huang, R., Wu, J., Chen, C. 2005. Influence of ggbs on durability and corrosion behavior of reinforced concrete. Materials Chemistry and Physics, 93, 404–411.

Crossin, E. 2015. The greenhouse gas implications of using ground granulated blast furnace slag as a cement substitute. Journal of Cleaner Production, 95, 101–108.

Eguchi, K., Takewaka, K., Yamaguchi, T., Ueda, N. 2013. A Study on durability of blast furnace slag cement concrete mixed with metakaolin-based artificial pozzolan in actual marine environment. Proceeding of Third International Conference on Sustainable Construction Materials and Technologies.

Garcia-Lodeiro, I., Palomo, A., Fernández-Jiménez, A. 2015. Crucial insights on the mix design of alkali-activated cement-based binders. handbook of alkali-activated cements, Mortars and Concretes, 49–73.

Grist, R., Paine, K., Heath, A., Norman, J., Pinder, H. 2015. The environmental credentials of hydraulic lime-pozzolan concretes. Journal of Cleaner Production, 93, 26–37.

Hamada, M., Thomas, B., Yahaya, F., Muthusamy, K., Yang, J., Abdalla, J., Hawileh, R. 2021. Sustainable use of palm oil fuel ash as a supplementary cementitious material: a comprehensive review. Journal of Building Engineering, 40, 102286.

Hawileh, R., Abdalla, J., Fardmanesh, F., Shahsana, P. 2017. Performance of reinforced concrete beams cast with different percentages of GGBS replacement to cement. Archives of Civil and Mechanical Engineering, 17, 511–519.

Huntzinger, D., Eatmon, T. 2009. A life-cycle assessment of Portland cement manufacturing: comparing the traditional process with alternative technologies. Journal of Cleaner Production, 17, 668–675.

Jeong, Y. Yum, W., Jeon, D., Oh, J. 2017. Strength development and microstructural characteristics of barium hydroxide-activated ground granulated blast furnace slag. Cement and Concrete Composites, 79, 34–44.

Joanna, P., Sangeetha, S. 2015. Flexural behaviour of reinforced concrete beams with partial replacement of GGBS. American Journal of Engineering Research, 3, 119–127.

Junaid, M.T., Karzad, A.S., Leblouba, M. 2020. Investigation on the properties of ambient cured alkali activated binder concrete. International Journal of Applied Science and Engineering, 18, 2020339

Karikalan, A., Prabaghar, A., Saravanan, J. 2021. Flexural behaviour of GGBS concrete beam with steel, hybrid FRP and GFRP bars. Turkish Journal of Computer and Mathematics Education, 12, 5719–5729.

Kyong Yon, Y., Kyum, K. 2005. An experimental study on corrosion resistance of concrete with ground granulate blast-furnace slag. Cement and Concrete Research, 35, 1391–1399.

Ma, C., Awang, A., Omar, W. 2018. Structural and material performance of geopolymer concrete: a review. Construction and Building Materials, 186, 90–102.

Mustafa, S., Hassan, H. 2018. Behavior of concrete beams reinforced with hybrid steel and FRP composites. HBRC Journal, 14, 300–308.

Nagaratnam, H., Rahman, M., Mirasa, A., Abdul Manan, M., Lame, S. 2016. Workability and heat of hydration of self-compacting concrete incorporating agro-industrial waste. Journal of Cleaner Production, 112, 882–894.

Nawaz, W. Abdalla, J., Hawileh, R., Alajmani, H. 2019. Experimental study on the shear strength of reinforced concrete beams cast with lava lightweight aggregates. Archives of Civil and Mechanical Engineering, 19, 981–996.

O'Connell, M., Mcnally, C., Richardson, M. 2012. Performance of concrete incorporating ggbs in aggressive wastewater environments. Construction and Building Materials, 27, 368–374.

Oner, A., Akyuz, S. 2007. An experimental study on optimum usage of GGBS for the compressive strength of concrete. Cement and Concrete Composites, 29, 505–514.

Ramakrishnan, K., Pugazhmani, G., Sripragadeesh, R., Muthu, D. 2017. Experimental study on the mechanical and durability properties of concrete with waste glass powder and ground granulated blast furnace slag as supplementary cementitious materials. Construction and Building Materials, 156, 739–749.

Samad, S., Shah, A. Limbachiya, M. 2017. Strength development characteristics of concrete produced with blended cement using ground granulated blast furnace slag (GGBS) under various curing conditions. Sādhanā, 42, 1203–1213.

Saranya, P., Nagarajan, P., Shashikala, A. 2018. Eco-friendly GGBS concrete: a state-of-the-art review. IOP Conference Series: Materials Science and Engineering, 330, 012057.

Siddique, R., Bennacer, R. 2012. Use of iron and steel industry by-product (GGBS) in cement paste and mortar. Resources, Conservation and Recycling, 69, 29–34.

Siddique, R., Bennacer, R. 2013. Utilization (recycling) of iron and steel industry by-product (GGBS) in concrete: strength and durability properties. Journal of Material Cycles and Waste Management, 16, 460–467.

Thomas, B., Yang, J., Mo, K., Abdalla, J. 2021. Biomass ashes from agricultural wastes as supplementary cementitious materials or aggregate replacement in cement/geopolymer concrete: a comprehensive review. Journal of Building Engineering, 40, 102332.

Topçu, I., Boğa, A. 2010. Effect of ground granulate blast-furnace slag on corrosion performance of steel embedded in concrete. Materials & Design, 31, 3358–3365.

Turner, L., Collins, F. 2013. Carbon dioxide equivalent (CO2-e) emissions: A comparison between geopolymer and OPC cement concrete. Construction and Building Materials, 43, 125–130.

Wan, H., Shui, Z., Lin, Z. 2004. Analysis of geometric characteristics of GGBS particles and their influences on cement properties. Cement and Concrete Research, 34, 133–137.

Wu, Y., Huang, R., Tsai, C., Lin, W. 2015. Recycling of sustainable co-firing fly ashes as an alkali activator for ggbs in blended cements. Materials, 8, 784-798.

Yuksel, I., 2018. Blast-furnace slag. Waste and Supplementary Cementitious Materials in Concrete, 361–415.